



Arab Academy for Science, Technology, and Maritime Transport

College of Engineering and Technology

Mechatronics Engineering

B. Sc. Final Year Project

PV Cleaning Robot

Presented By:

Reham Eid

19106651

Supervised By:

Dr. Sameh Shaaban

DECLARATION

I hereby certify that this material, which I now submit for assessment on the program of study leading to the award of Bachelor of Science in *Mechatronics Engineering* is entirely my work, that I have exercised reasonable care to ensure that the work is original, and does not to the best of my knowledge breach any law of copyright, and has not been taken from the work of others save and to the extent that such work has been cited and acknowledged within the text of my work.

Signed: Reham Eid

Registration No.: 19106651

Date: 1 Monday, January 2024

Table of Contents

1	introduction	1
2	simulation (simulink)	3
2.1	introduction.....	3
2.2	system overview	3
2.3	converting Solidworks to Simscape	3
2.4	Simulink model.....	4
2.4.1	Creating the motor subsystem	4
2.4.2	Simulate all revolute joints with the chosen motor	8
2.4.3	Faced problems and solving methods.....	9
2.4.4	IMU sensor integration.....	11
2.5	simulation and results	13
2.5.1	First Trial - Motor Selection:.....	13
2.5.2	Second Trial - Motor Integration:.....	13
2.5.3	Third Trial - IMU Sensor Integration:	13
2.6	conclusion	13
3	code & circuit	15
3.1	components	15
3.1.1	PCB design	15
4	Conclusion	17
4.1	conclusion	17

List of figures

Figure 1: map of the areas with the highest dust amount.....	1
Figure 1: generated simscape model.....	4
Figure 2: subsystem of the motor.	5
Figure 3: data of the motor of the brush.	6
Figure 4: motor data.	7
Figure 5: simulate all revolutes with the chosen motor.	7
Figure 6: simulation of the system with the chosen motors.....	8
Figure 7: display of output torque and velocity of brush.	8
Figure 8: scope for the driving motors.....	9
Figure 9: result of velocity increased to infinite.	9
Figure 10: error message in diagnostic viewer.	10
Figure 11: damping coefficient of revolute.	10
Figure 12: matlab function block.....	11
Figure 13: Results of the wheel speed when output is -25.....	12
Figure 14: Result of the wheel speed when output is larger than -25.	12
Figure 15: Result of the wheel speed when output is smaller than -25.....	12
Figure 16: PCB layout.	16

Chapter One

1 INTRODUCTION

In recent years, there has been a significant increase in power generation from renewable sources, driven by rising energy demand and growing concerns about the environmental and economic impact of fossil fuels. Among these sources, photovoltaic (PV) energy stands out as having immense future potential due to its simple installation, high reliability, low maintenance costs, and zero fuel expenses.

Solar photovoltaic energy is derived from solar radiation, and under standard test conditions, only 15-18% of solar radiation is effectively converted into electricity by a monocrystalline solar PV panel. Despite the challenges in achieving maximum efficiency, such as variations in irradiance, air mass, and temperature, the primary hindrance to harnessing solar radiation is the accumulation of foreign particles like dust, bird excrement, and snow.

Solar panels are expected to be beneficial in Egypt due to the country's high level of solar radiation and lengthy periods of daily sunlight throughout the year. Here, the average solar energy production as of the year 2022 is 1724 megawatts in Egypt. This represented a 3.67% increase compared to the past year (2021). It is anticipated that Egypt will invest over 6.5 billion/year to achieve its goals of producing more renewable energy. To maintain the effectiveness of the PV panels, Egypt has two significant challenges: high ambient temperature and prevailing dust storms in the desert region, as shown in Figure 1. This factor reduces PV panel production and thus must be kept below specific levels. Considering the adverse effect of dust accumulation on PV panels, there have been significant effects to discover ways and means to clean the PV panels without ruining their surface.

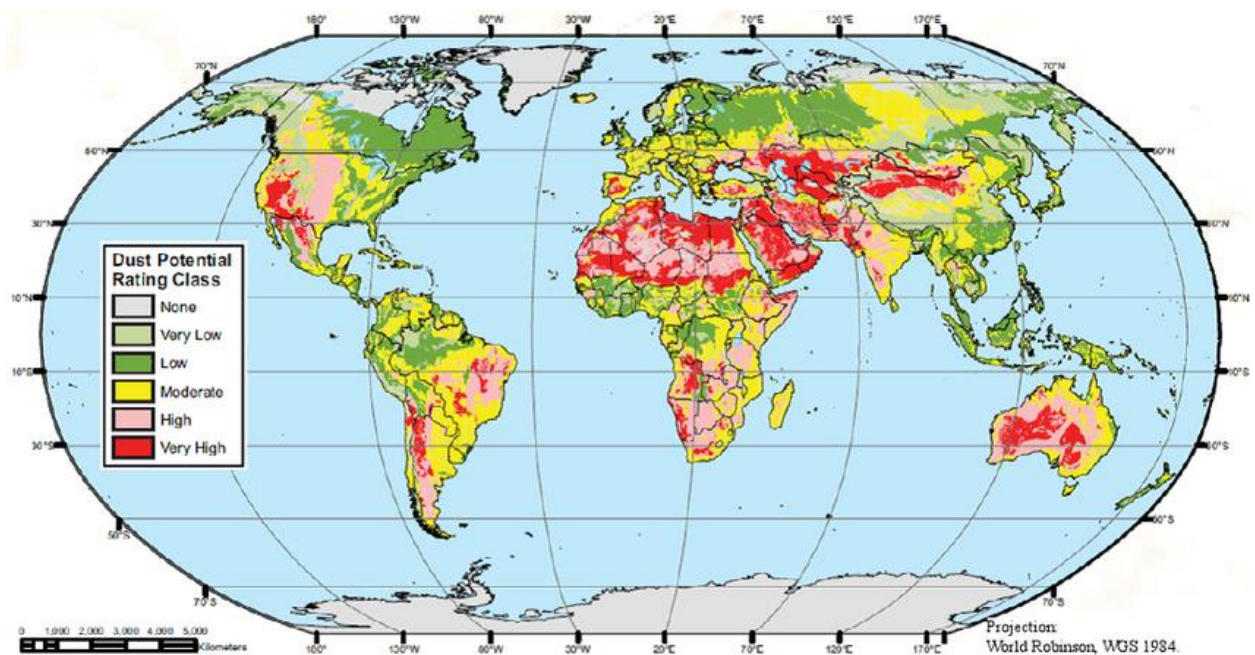


Figure 1: map of the areas with the highest dust amount.

The dust accumulation on the surface of the solar panels hampers their ability to receive solar energy, leading to a reduction in the efficiency of PV panels by up to 40%. The frequent incidence of dust storms, coupled with humidity, results in manual cleaning methods requiring skilled personnel to operate the equipment intelligently while ensuring that the panels' surface remains undamaged. Additionally, the cleaning of extensive PV farms in harsh weather conditions can significantly impact the health of employees.

Most of the currently available technologies for cleaning solar PV panels in desert environments, such as Egypt, rely on only water, which is scarce and expensive. Furthermore, periodic cleaning of solar panels, depending on the level of dust, consumes a substantial amount of water, ultimately increasing the cost. Modern systems utilize autonomous robots, which are slow and require always water for surface cleaning, rendering them unsuitable for large-scale PV plants in Egypt and other regions with similar climates. The proposed method of cleaning solar PV panels is by using a fully automated cleaning system. This system is coded to be able to decide by itself which type of cleaning method is more efficient at the moment, whether it's with water or without water, can check the effectiveness of the cleaning, and has a clock to decide which time of the day is more suitable for the cleaning. This system is the most we know that is a cost-effective, timesaving, and water-efficient solution. This project aims to try to solve the problem of dust accumulation in Egypt and boost the efficiency of the energy generated by solar PV panels with less water as much as possible.

2 SIMULATION (SIMULINK)

2.1 INTRODUCTION

In this section, we present the implementation of our fully automated AI-assisted PV cleaning system using Simulink. Simulink provides a simulation environment that enables us to model and test the movement of our system, which comprises five motors: four motors responsible for the wheels' movement across the PV panel, and one motor for the brush that cleans the panel.

Our strategy encompasses several stages of simulation trials in Simulink. In the first trial, we aimed to identify the most efficient motors from those available locally. We obtained datasheets for various motors, simulated their performance in terms of speed and torque, and selected the most suitable ones for our system. In the second trial, we integrated the selected motors to ensure that the system moved optimally. Finally, the third trial involved integrating the system with the IMU sensor to dynamically adjust the motor speed based on the sensor readings, resulting in efficient and adaptive movement.

2.2 SYSTEM OVERVIEW

Our photovoltaic (PV) cleaning system was designed to autonomously traverse solar panels while adjusting their movement based on data from an inertial measurement unit (IMU) sensor. The IMU sensor readings dictate the speed and direction of the motors, thereby ensuring optimal cleaning performance. The primary components of our system are as follows:

1. Four motors for wheel movement.
2. One motor for the cleaning brush.
3. An IMU sensor for detecting the system's orientation and movement.

2.3 CONVERTING SOLIDWORKS TO SIMSCAPE

SolidWorks will Generate STEP file and XML file which a documentation that documents Orientation, Position, Colours and mates of each part within assembly.

We convert .xml File into simscape Multibody(.slx) through a command which is:
`smimport("assembly_one","ModelName","PV_Cleaning_Data","DataFileName","PV_Cleaning_DataFile");`

where, assembly_one is the name of xml file which I need to convert to simscape and it should find in the same path of assembly

"PV_Cleaning": it's the name that will appear in Simulink Model generated

"PV_Cleaning_DataFile": it's a .m file generated to save data of assembly in it.

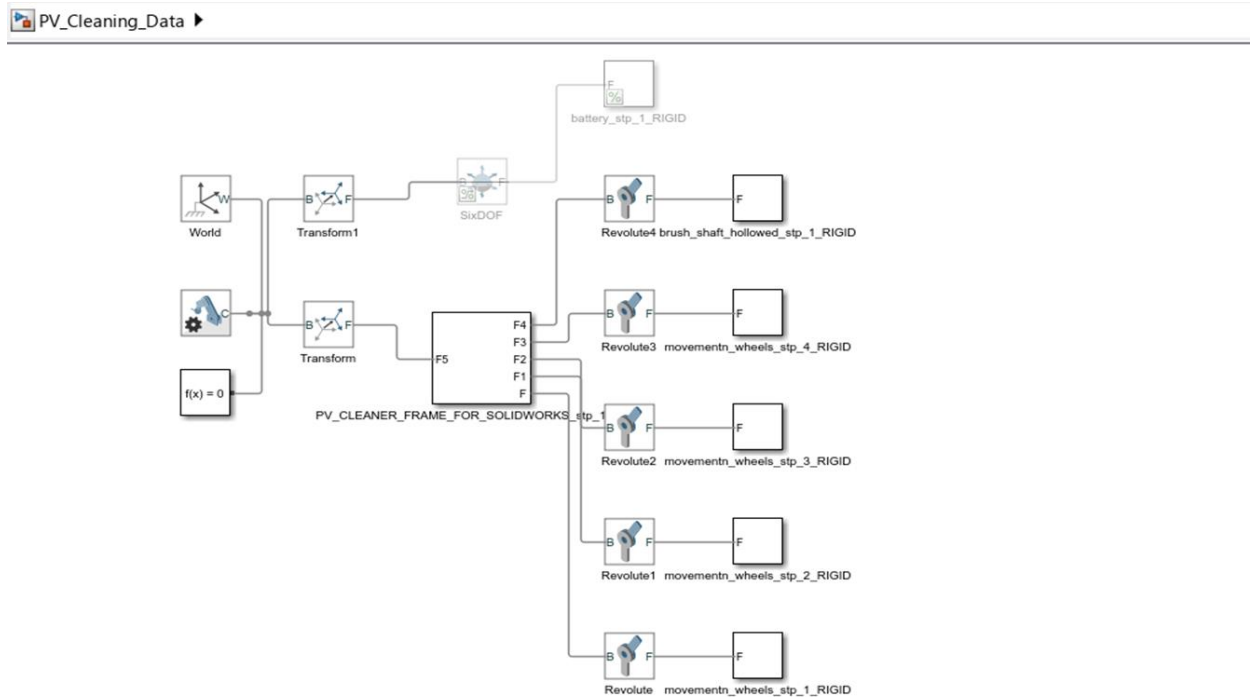


Figure 2: generated simscape model.

2.4 SIMULINK MODEL

2.4.1 Creating the motor subsystem

In Simulink, we developed a subsystem for motors with the connected revolute to try several motors that can be purchased Locally and Move the system with the best Performance.

We obtained datasheets for motors readily available in the local market and utilized Simulink to simulate their performance. The simulations were focused on assessing the output speed and torque of the motors to determine the most suitable ones for the proposed system. The selected motors provided the optimal combination of speed and torque necessary for efficient system operation.

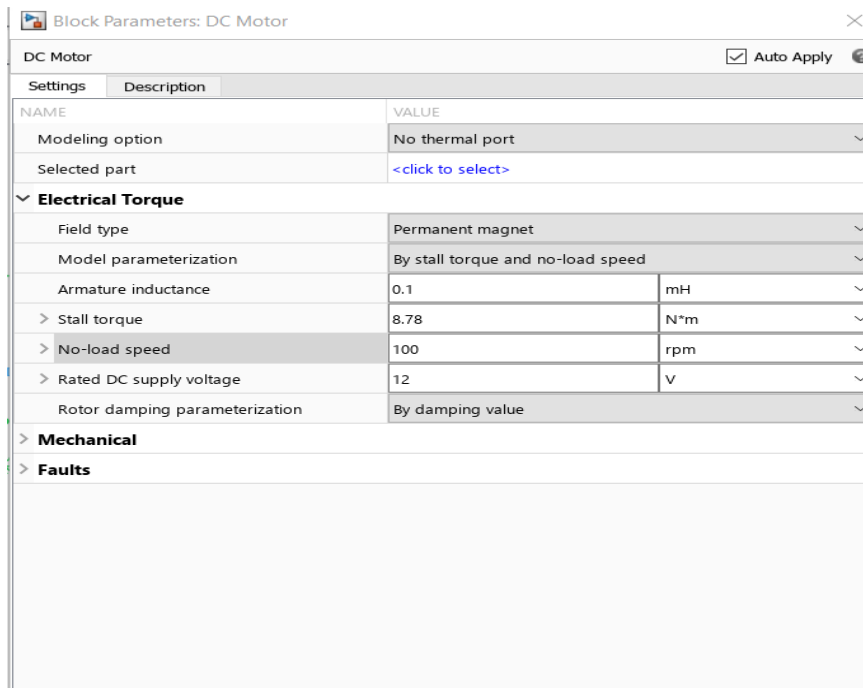
The source is ideal in the sense that it is assumed to be powerful enough to maintain a specified velocity regardless of the torque exerted on the system.

It consists of ports:

- S** — Control signal: Physical signal input port, through which the control signal that drives the source is applied.
- R** — Rod: Mechanical rotational conserving port associated with the source moving part (rod).
- C** — Case: Mechanical rotational conserving port associated with the source reference point (case).

Chosen Motors for System: DC Geared Motor 12VDC 125 RPM 1.86 N.M

Chosen Motor for brush: 12V 100 RPM used to rotate the brush, used for the high torque 8.78



Block Parameters: DC Motor

DC Motor ☒ Auto Apply

NAME	VALUE
Modeling option	No thermal port
Selected part	<click to select>
Electrical Torque	
Field type	Permanent magnet
Model parameterization	By stall torque and no-load speed
Armature inductance	0.1 mH
> Stall torque	8.78 N*m
> No-load speed	100 rpm
> Rated DC supply voltage	12 V
Rotor damping parameterization	By damping value
> Mechanical	
> Faults	

Figure 4: data of the motor of the brush.

Block Parameters: DC Motor3
✕

DC Motor
☒ Auto Apply
?

SettingsDescription

NAME	VALUE
Modeling option	No thermal port
Selected part	<click to select>
Electrical Torque	
Field type	Permanent magnet
Model parameterization	By stall torque and no-load speed
Armature inductance	1.35
> Stall torque	1.86
> No-load speed	5000
> Rated DC supply voltage	12
Rotor damping parameterization	
No-load current	600
> DC supply voltage when measuring no-lo...	12
Mechanical	
Faults	

Figure 5: motor data.

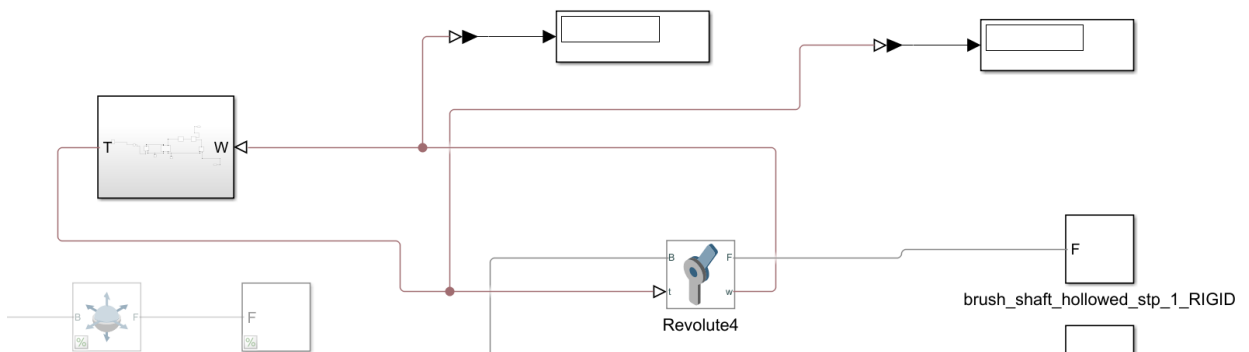


Figure 6: simulate all revolute with the chosen motor.

2.4.2 Simulate all revolutes with the chosen motor

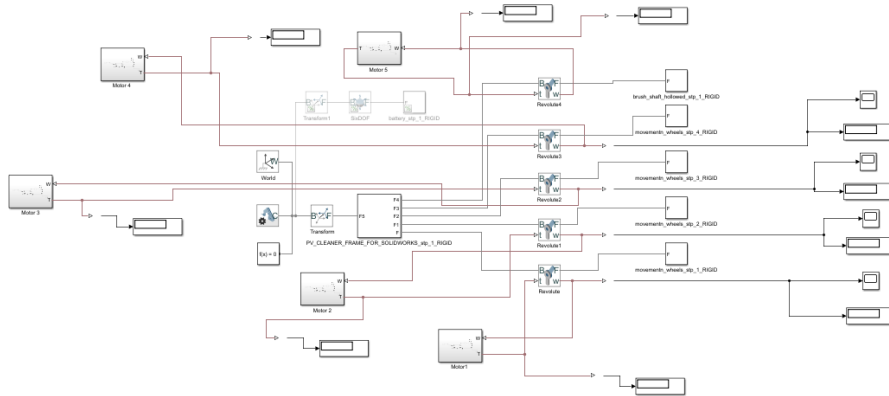


Figure 7: simulation of the system with the chosen motors.

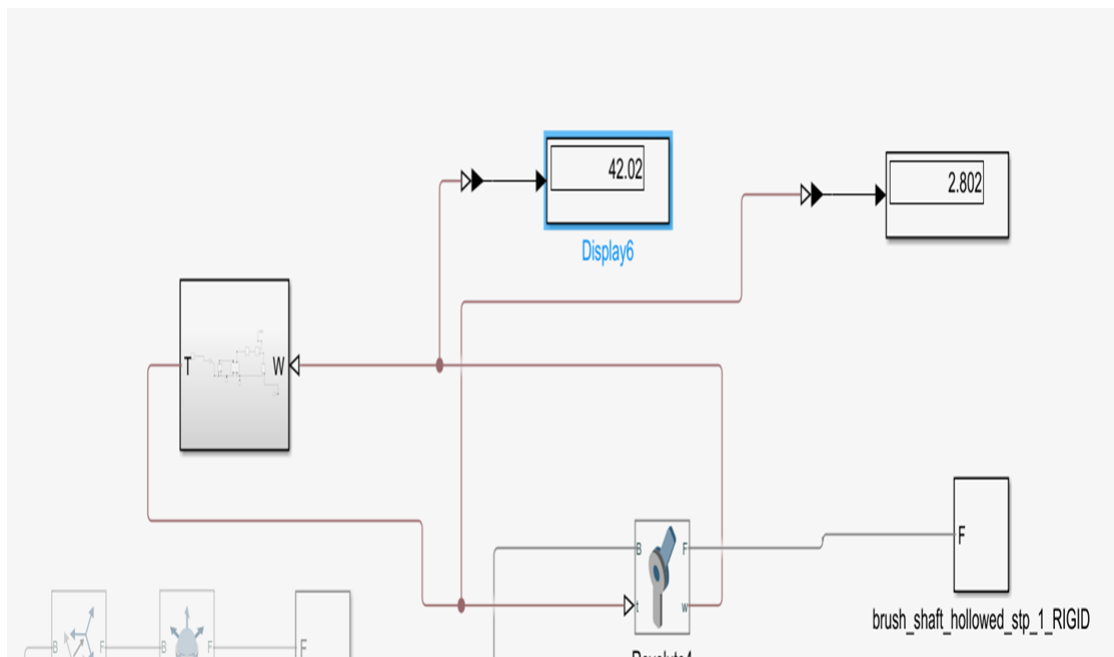


Figure 8: display of output torque and velocity of brush.

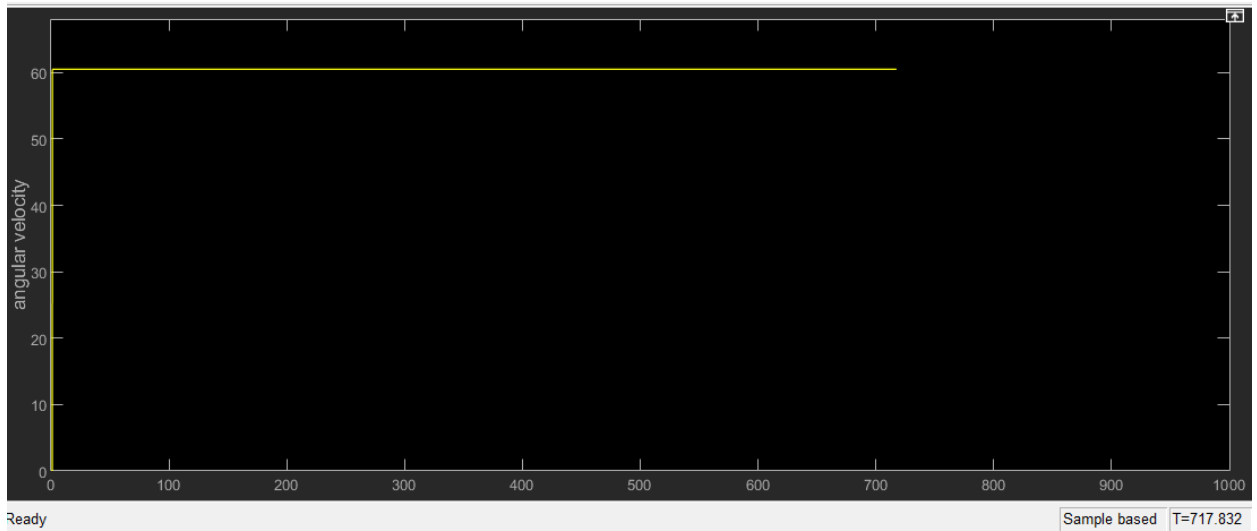


Figure 9: scope for the driving motors.

2.4.3 Faced problems and solving methods

First problem: simulation was terminated as it's Failed to satisfy dynamic state constraints.

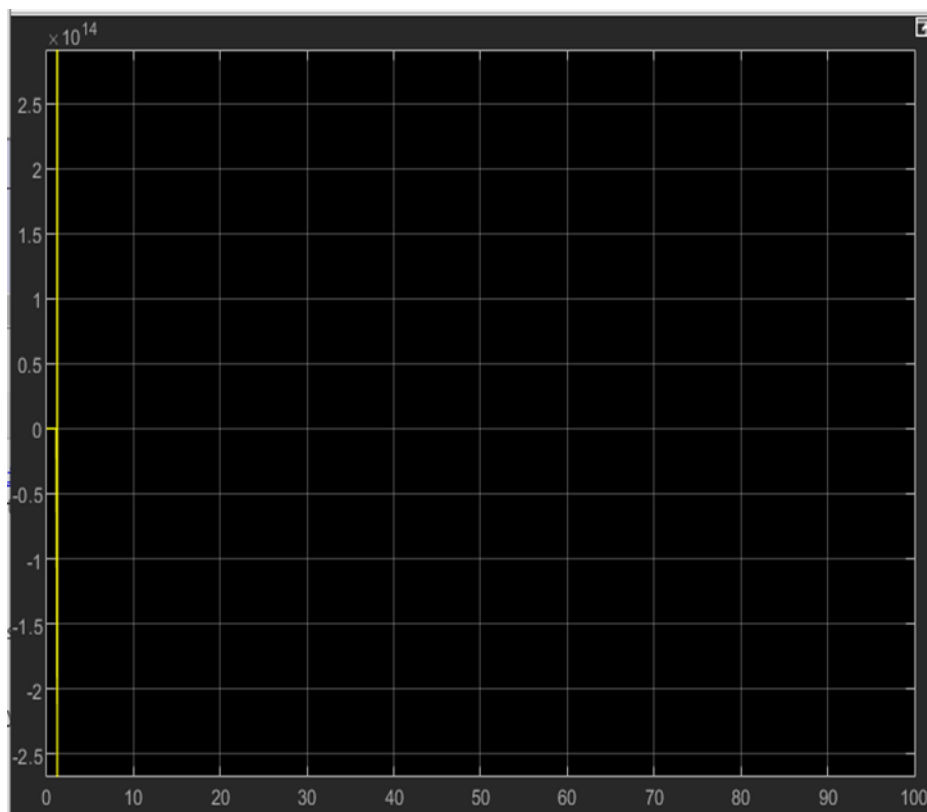


Figure 10: result of velocity increased to infinite.

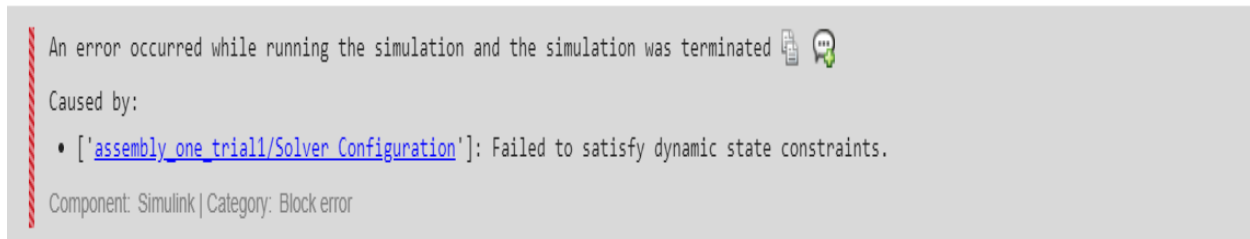


Figure 11: error message in diagnostic viewer.

Solving methods of problem:

1- Changing Unit in PS_Simulink converter depending on the scope it shows

For Example:

- If it going to scope of torque we changed unit to $N \cdot m$.
- If it going to scope of Velocity we changed unit to rpm.
- If it going to scope of Volt we changed unit to V.

2- Increase damping Coefficient of revolute to 0.111113 and we used this number trough several trials in which it doesn't affect the output of revolute also to solve the problem.

Settings	Description		
NAME	VALUE		
▼ Z Revolute Primitive (Rz)			
> State Targets			
▼ Internal Mechanics			
Equilibrium Position	0	deg	▼ Compile-time ▼
Spring Stiffness	0	N*m/deg	▼ Compile-time ▼
Damping Coefficient	0.0111113	N*m/(deg/s)	▼ Compile-time ▼
> Limits			
▼ Actuation			
Torque	Provided by Input ▼		
Motion	Automatically Computed ▼		
> Sensing			

Figure 12: damping coefficient of revolute.

2.4.4 IMU sensor integration

The Inertial Measurement Unit (IMU) sensor is a critical component in the robotic vehicle as it provides orientation data that is necessary for adjusting the speed of the wheel motors. In Simulink, the IMU sensor was modeled using a custom block that outputs a range of values representing the readings from the sensors.

IMU Sensor Block:

1. The Knobe block outputs a signal representing the IMU sensor reading, which ranges from -40 to -9.
2. This signal is used to control the speed of the wheel motors.

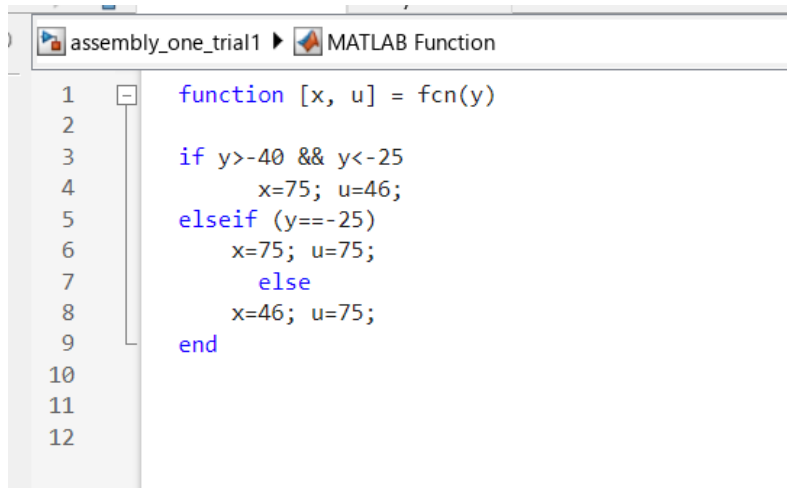


Figure 13: matlab function block.

The IMU sensor range was divided into three segments: [-40, -26], [-25], and [-24, -9]. For each range, the corresponding motor speeds were set as follows:

1. Range [-40, -26]: Motor1 and Motor2 run at 38 rpm, whereas Motor3 and Motor4 run at 62.5 rpm.
2. Range [-25]: All four motors were operated at 62.5 rpm.
3. Range [-24, -9]: Motor1 and Motor2 run at 62.5 rpm, whereas Motor3 and Motor4 run at 38 rpm.
4. The IMU sensor output is fed into a MATLAB Function block, which contains the control logic that outputs the appropriate motor speeds. The motor speed outputs are connected to the respective DC Motor blocks for Motor1 to Motor4.

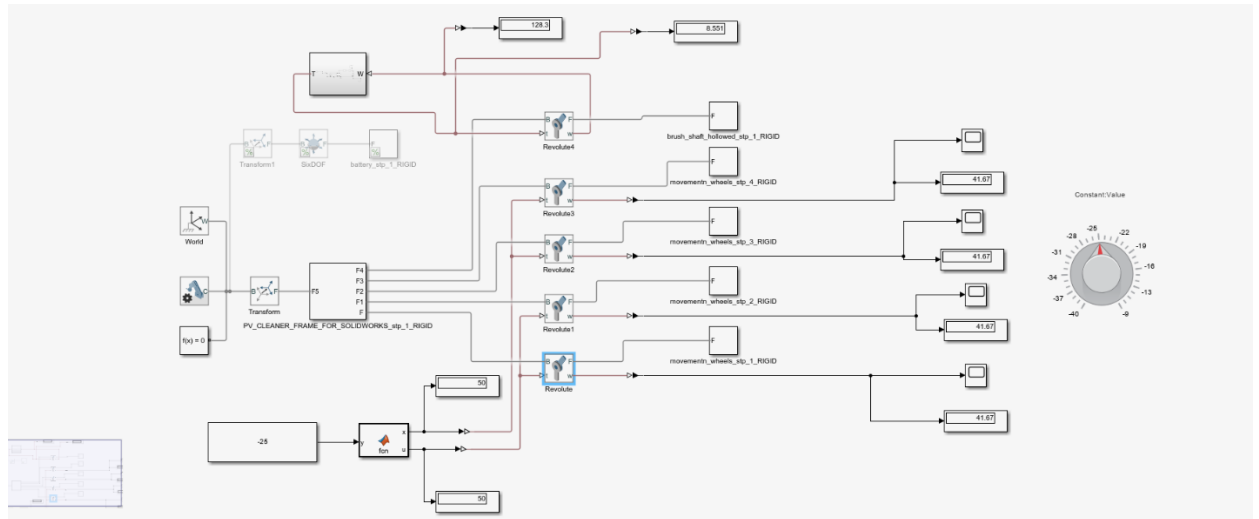


Figure 14: Results of the wheel speed when output is -25.

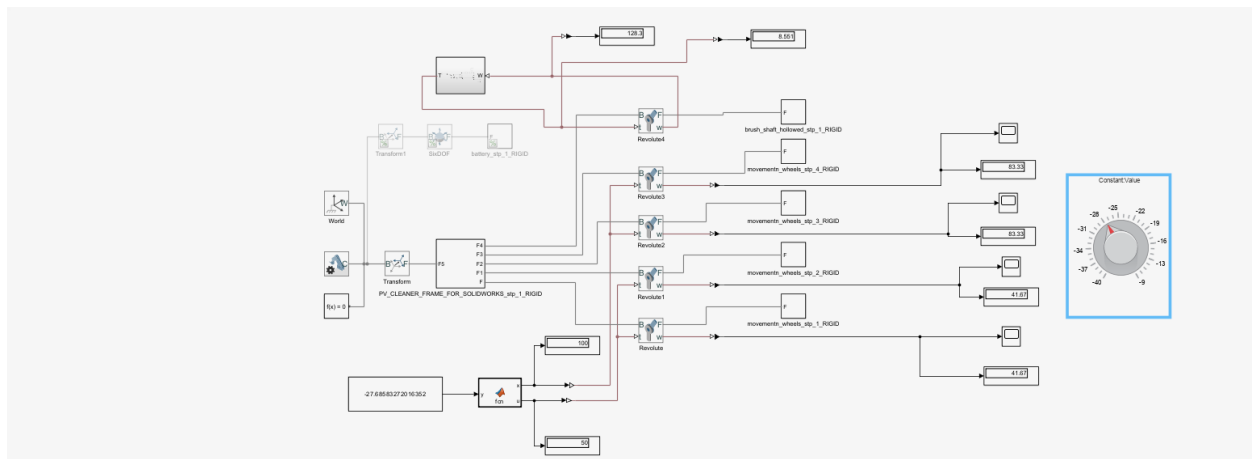


Figure 15: Result of the wheel speed when output is larger than -25.

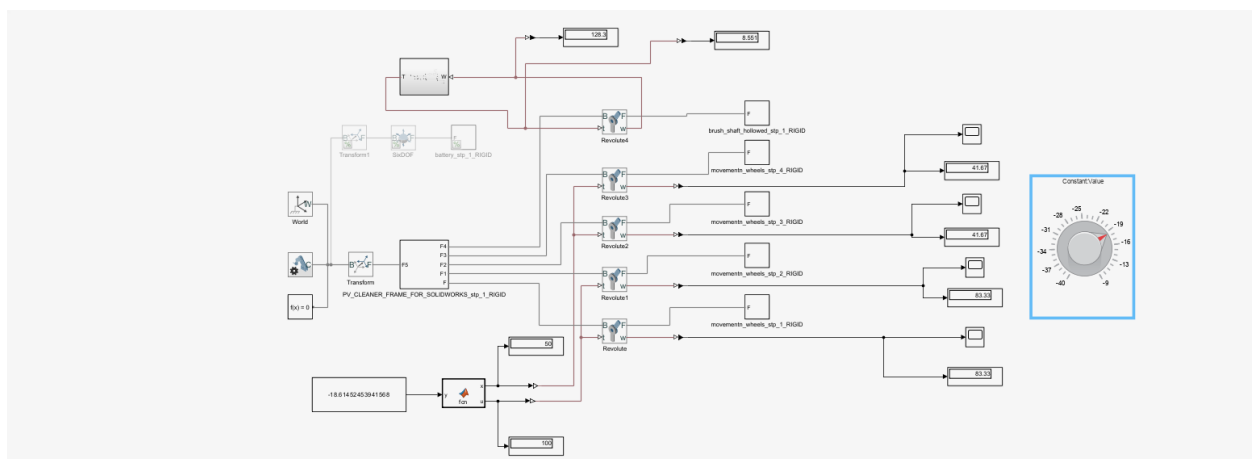


Figure 16: Result of the wheel speed when output is smaller than -25.

2.5 SIMULATION AND RESULTS

The simulation results demonstrated that the robotic vehicle was able to navigate through the obstacle course successfully, with the control logic effectively adjusting the motor speeds based on the IMU sensor readings. The vehicle was able to maintain a stable speed and make smooth turns, demonstrating the effectiveness of the control logic implementation.

Upon completion of the implementation, we conducted simulations to verify the functionality of the system across multiple trials.

2.5.1 First Trial - Motor Selection:

We obtained datasheets for motors readily available in the local market and utilized Simulink to simulate their performance. The simulations were focused on assessing the output speed and torque of the motors to determine the most suitable ones for the proposed system. The selected motors provided the optimal combination of speed and torque necessary for efficient system operation.

2.5.2 Second Trial - Motor Integration:

We integrated the selected motors into the system to ensure coordinated movement.

The simulations confirmed that the motors worked seamlessly together, delivering smooth and synchronized movement across the PV panels.

2.5.3 Third Trial - IMU Sensor Integration:

- We integrated the IMU sensor with the system to enable dynamic adjustment of motor speed based on sensor readings.
- The simulations validated the control logic, demonstrating that the motors responded correctly to the IMU sensor data, adjusting their speeds following the defined logic.
- The key observations from the simulations are as follows:
- When the IMU sensor readings were between -40 and -26, Motor1 and Motor2 ran at 38 rpm, while Motor3 and Motor4 ran at 62.5 rpm.
- When the IMU sensor reading was exactly -25, all four motors operated at 62.5 rpm.
- When the IMU sensor readings were between -24 and -9, Motor1 and Motor2 ran at 62.5 rpm, while Motor3 and Motor4 ran at 38 rpm.
- These results illustrate that the system can dynamically adjust its movement based on IMU sensor data, ensuring efficient and adaptive navigation across the PV panels.

2.6 CONCLUSION

This section details the implementation of our automated PV cleaning system in Simulink. By modeling the motors and integrating the IMU sensor, we were able to simulate and validate the system performance across multiple trials. The first trial helped us select the best-performing motors, the second trial ensured that their integration provided optimal system performance, and the third trial confirmed that the system dynamically adjusted the motor speeds based on IMU

sensor readings. These simulations lay the groundwork for the physical implementation and further.

3 CODE & CIRCUIT

3.1 COMPONENTS

3.1.1 PCB design

They were designed and developed a custom PCB shield for the Arduino Mega that facilitates the integration of various sensors and modules. This shielding is intended to optimize the connections and ensure efficient communication between the Arduino and the peripheral components. The shield includes connectors for two ultrasonic sensors, an Inertial Measurement Unit (IMU), three motor drivers, a Bluetooth module, an LCD, and an environmental sensor. The design and layout of the PCB were carried out using the Easy EDA tool, a powerful and easy-to-use electronic design automation software.

The first step was to create the schematic diagram in Easy EDA. After the schematic was completed, the next step was to design the PCB layout. The Easy EDA tool efficiently arranged components and route traces, ensuring minimal interference and optimal signal integrity.

- 1- Layer Structure: A Single-layer PCB was chosen to manage the complexity of routing.
- 2- Component Placement: Components were strategically placed to minimize trace lengths and avoid crossing signals.
- 3- Routing: Traces were routed to ensure clear and direct paths, especially for high-frequency signals and power lines. Ground planes were used extensively to reduce noise and provide stable grounding.

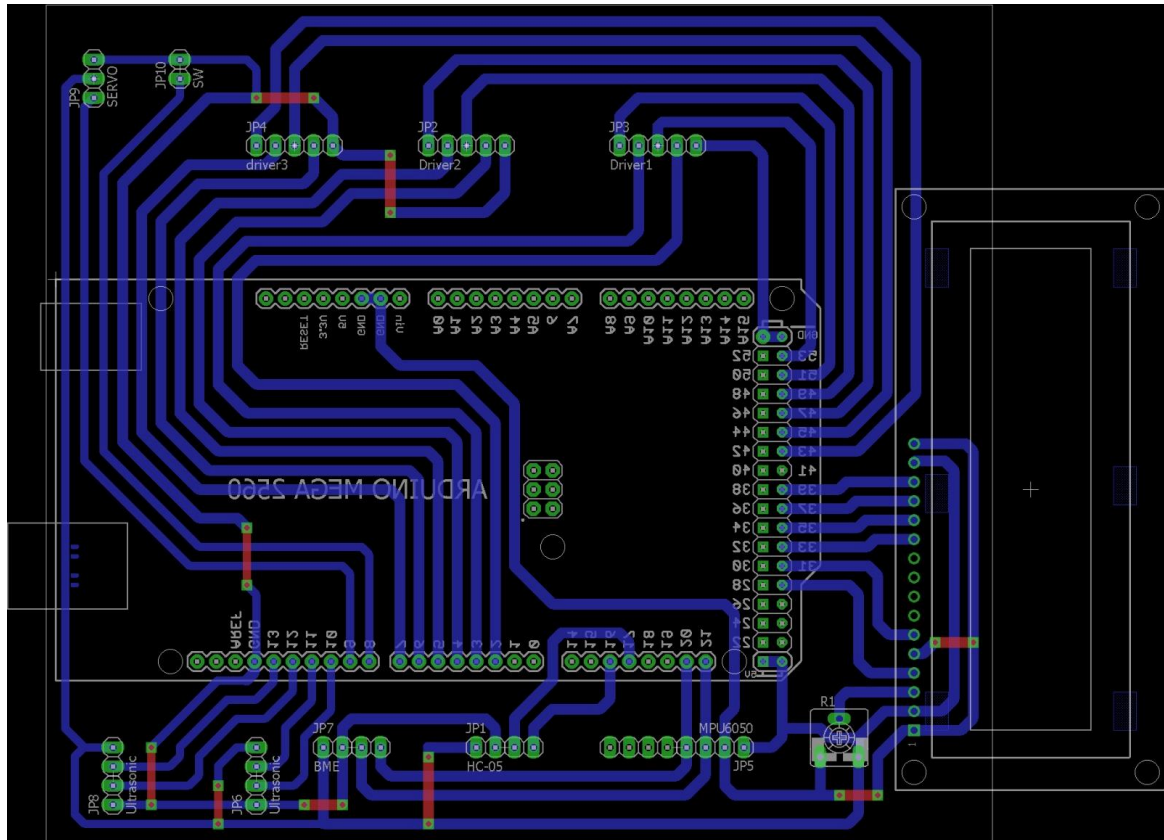


Figure 17: PCB layout.

The final PCB shield has successfully integrated all the specified components into the Arduino Mega. Tests confirmed that all sensors and modules worked as intended and met the project objectives. Using the Easy EDA tool streamlined the design process and enabled efficient schematic capture and PCB layout. Challenges during the design phase included managing trace routing for the dual-layer PCB and ensuring signal integrity for high-frequency signals. These issues were addressed through careful planning and iterative design improvements.

Chapter four

4 CONCLUSION

4.1 CONCLUSION

In conclusion, the increasing global demand for renewable energy, particularly from photovoltaic sources, has led to a surge in solar power generation. Egypt, with its abundant solar radiation and ambitious renewable energy goals, is poised to capitalize on solar energy production. However, the region faces unique challenges, notably the impact of high ambient temperatures and frequent dust storms on the efficiency of solar PV panels.

The research underscores the critical issue of dust accumulation on solar panels, highlighting its detrimental effects on energy production efficiency. Existing cleaning methods, often reliant on water in arid environments like Egypt, pose economic and environmental challenges. The proposed fully automated cleaning system emerges as a promising solution, offering a cost-effective, timesaving, and water-efficient approach to maintaining the effectiveness of PV panels.

As Egypt invests significantly in renewable energy projects, the success of this project could contribute substantially to achieving the country's renewable energy targets. By addressing the challenges posed by dust accumulation in solar PV panels, the automated cleaning system not only enhances energy production efficiency but also minimizes the reliance on scarce water resources. As it's a fully automated system using AI that makes decisions for the cleaning process whether to clean it or not and to clean it dry or using water also, it sizes itself according to the size of the panel.

This research endeavors to pave the way for sustainable and efficient solar energy production in Egypt and similar climates, ultimately advancing the global transition to cleaner and more sustainable energy sources.

